MATERIALE PLASTICE
https://revmaterialeplastice.ro
https://doi.org/10.37358/Mat.Plast.1964

A Chitosan/Oxidized Pullulan Composite Film for Localized Cisplatin Delivery and *In Vitro* Evaluation on Nasopharyngeal Cells

BING CAO*, SHANSHAN GU, YI HU, YUNA ZHANG
Department of Otolaryngology-Head and Neck Surgery, The Affiliated Lihuili Hospital of Ningbo University, Ningbo, 315040, China

Abstract: ***Background:*** *Postoperative wound sealing and localized drug delivery are critical needs in nasopharyngeal carcinoma (NPC) management. Natural polysaccharide-based films offer a biocompatible platform for addressing these challenges.* ***Methods:*** *A composite film was prepared by Schiff base crosslinking of chitosan and oxidized pullulan. The film was characterized by FTIR, and its adhesion, drug release, cytocompatibility, and effects on cell migration were evaluated using in vitro assays.* ***Results:*** *The composite film exhibited a distinct C=N peak in FTIR spectra and significantly enhanced wet adhesion (55 kPa) compared to individual components. Cisplatin-loaded films showed sustained release over 72 h and reduced the viability of CNE-2 cells to 28%. The drug-free film was non-cytotoxic. Extracts from the composite film promoted nasopharyngeal epithelial cell migration, as shown by RTCA assay.* ***Conclusion:*** *This study explored the in vitro characteristics of a chitosan/oxidized pullulan film and evaluated its basic biological performance at the cellular level capable of localized drug release and supporting cell-level healing responses. Further validation in more complex models is warranted.*

Keywords: *Chitosan, oxidized pullulan, composite film, cisplatin delivery, epithelial migration*

1. Introduction

Nasopharyngeal carcinoma (NPC) is a malignant tumor originating from the epithelial lining of the nasopharynx, with a high incidence in Southeast Asia and southern China. Surgical resection, often combined with radiotherapy and chemotherapy, remains a key component of treatment [1,2]. However, postoperative tissue injury, risk of tumor recurrence, and challenges in local drug delivery complicate the recovery process [3,4]. Developing biomaterials that integrate wound sealing and localized drug delivery functions has attracted growing research interest, particularly at the preclinical exploratory level [5–7].

Chitosan is a natural polysaccharide known for its biocompatibility, biodegradability, and moderate bioadhesive properties. Oxidized polysaccharides, such as oxidized pullulan, can introduce aldehyde groups capable of forming dynamic covalent bonds with amino-functional materials [8,9]. When crosslinked via Schiff base chemistry, these components can form stable, bioadhesive films with potential utility in wound management and localized therapy [10]. While previous studies have reported on the material properties of such systems, their specific influence on cellular behaviors—such as cancer cell inhibition and epithelial cell migration—has been less systematically explored [11,12].

In this study, we focused on the early-stage evaluation of a chitosan/oxidized pullulan composite film from a cellular perspective. Rather than pursuing comprehensive *in vivo* assessments, we aimed to clarify how this material interacts with two key cell types: nasopharyngeal carcinoma cells and epithelial cells involved in wound repair. By combining basic chemical characterization with drug release, cytotoxicity, and migration assays, our goal was to assess whether the film offers functional support for localized cisplatin delivery while maintaining cytocompatibility and potentially facilitating epithelial regeneration. Though preliminary, this cell-centered investigation provides foundational

email: cbb7417@163.com

insight into the dual biological performance of the material and lays the groundwork for more complex future evaluations.

2. Methods

Chitosan (medium molecular weight, deacetylation degree ≥ 85%) and pullulan were purchased from commercial suppliers. Sodium periodate, cisplatin, and other analytical-grade reagents were used as received. Oxidized pullulan was prepared by reacting pullulan with sodium periodate (molar ratio 1:1.5) in the dark at 4°C for 12 h, followed by dialysis and freeze-drying.

2.1. Preparation of composite film

Chitosan was dissolved in 1% acetic acid (2% w/v), and oxidized pullulan was dissolved in deionized water (2% w/v). Equal volumes of the two solutions were mixed and cast into Petri dishes, allowing Schiff base crosslinking to occur at room temperature for 24 h. Films were then dried under vacuum and stored for further testing.

2.2. FTIR spectroscopy

Dried samples of chitosan, oxidized pullulan, and the composite film were ground with KBr and pressed into pellets. FTIR spectra were recorded using a spectrometer in the range of 4000–500 cm^{-1} at a resolution of 4 cm^{-1}. All spectra were normalized to their respective maximum absorbance to facilitate peak comparison.

2.3. Lap-shear adhesion test

Fresh sausage casing was cut into strips (2 cm × 5 cm) and used as a moist biological substrate. Each film sample was placed between two overlapping casing strips (1 cm^2 overlap area). The assembly was pressed and left for 10 min under light pressure. Lap-shear tests were conducted using a universal testing machine at a speed of 5 mm/min. Maximum shear stress before failure was recorded. Five replicates were tested for each group.

2.4. *In vitro* drug release study

The release samples were subsequently re-analyzed by inductively coupled plasma mass spectrometry (ICP-MS) to quantify platinum content. The ICP-MS data confirmed the same overall release trend with improved accuracy, and these updated results are presented in Figure 1. At each predetermined time point (1, 4, 8, 12, 24, 48, and 72 h), 1 mL of PBS release medium was collected and diluted as needed. The Pt concentration (C_t, in μg/mL) was determined using an external standard calibration method. Since each cisplatin molecule contains one Pt atom, the measured Pt content was converted to the equivalent mass of cisplatin using the molecular weight ratio (cisplatin: Pt = 300.05:195.08). The cumulative release percentage at each time point was calculated using the following formula:

$$\text{Release Rate}_t\,(\%) = \frac{C_t \cdot V \cdot \dfrac{300.05}{195.08}}{M_0} \times 100\%$$

where V is the volume of the release medium (5 mL), and M_0 is the total initial amount of cisplatin loaded in each sample. All measurements were performed in triplicate.

2.5. Cell viability assay

Nasopharyngeal carcinoma CNE-2 cells were seeded in 96-well plates at a density of 5000 cells/well. After 24 h, the medium was replaced with film extract solutions (prepared by soaking 1 cm^2 of film in 1 mL serum-free medium for 24 h). Groups included control (no treatment), free cisplatin (5 μg/mL), drug-free composite film extract, and cisplatin-loaded film extract. The control group consisted of cells cultured in complete medium without any exposure to drug, film extract, or vehicle. This group was

used to establish baseline cell viability for comparison with treated groups. After 48 h incubation, cell viability was measured using the CCK-8 assay, and absorbance at 450 nm was read using a microplate reader. The "drug-free composite film" group was prepared under the same Schiff base crosslinking conditions as the cisplatin-loaded film, using chitosan and oxidized pullulan without cisplatin. This group was included specifically to evaluate the cytocompatibility of the crosslinked matrix and its degradation products alone.

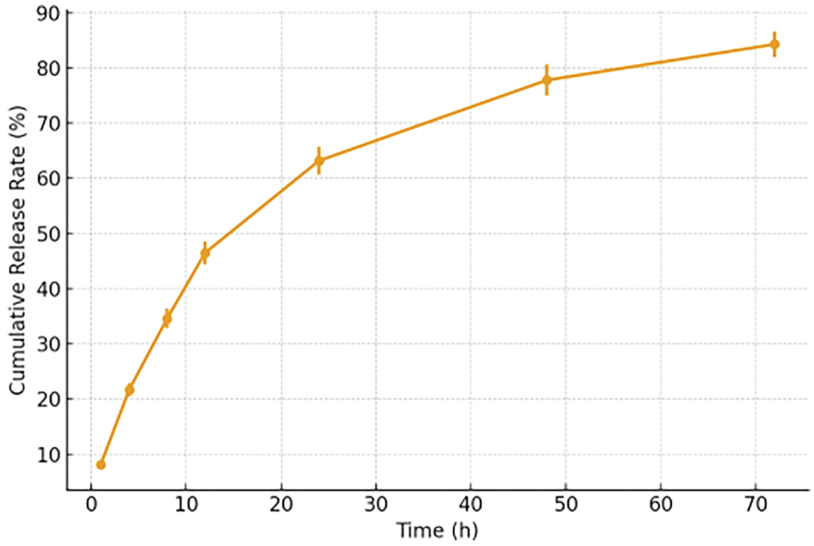

Figure 1. Cumulative release profile of cisplatin from the composite film over 72 h. Drug release was measured in PBS at 37°C, with results expressed as mean ± standard deviation (n = 3)

2.6. Real-time cell migration assay

Human nasopharyngeal epithelial NP69 cells were seeded in CIM-plate 16 inserts (xCELLigence RTCA system) at 2×10^4 cells/well in serum-free medium. The lower chamber contained film extract diluted 1:1 with complete medium as a chemoattractant. Cell index (CI) was recorded every 15 min for 48 h. Groups included control, oxidized pullulan extract, chitosan extract, and composite film extract. Final CI values and curve slopes were used to evaluate migration behavior.

Statistical analysis was performed using one-way analysis of variance (ANOVA) followed by Tukey's post hoc test to assess differences between groups. All data are presented as mean ± standard deviation (n = 3). A p-value less than 0.05 was considered statistically significant. The following notation was used to indicate significance levels: $p < 0.05$ (*), $p < 0.01$ (**), and $p < 0.001$ (***). All statistical analyses were performed using GraphPad Prism 9.0 (GraphPad Software, San Diego, CA, USA).

3. Results

As shown in Figure 2, a schematic diagram was constructed to illustrate the formation and application of the chitosan/oxidized pullulan composite adhesive film. The molecular structure of chitosan highlights the presence of amino groups, which react with the aldehyde groups in oxidized pullulan to form Schiff base (C=N) linkages, resulting in a chemically crosslinked network. This network is depicted as a film structure capable of adhering to moist tissue surfaces. The figure further demonstrates the application of the film to the postoperative site of nasopharyngeal carcinoma, where it serves a dual function—sealing the wound and delivering cisplatin locally. The schematic indicates that the drug-loaded film remains *in situ* and gradually releases cisplatin over time to achieve localized

chemotherapy. This figure supports the design rationale for a multifunctional bioadhesive film with both mechanical sealing and therapeutic delivery capabilities.

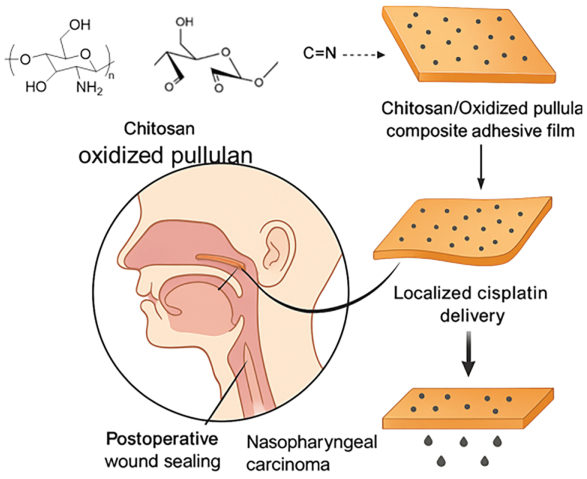

Figure 2. Schematic illustration of the chitosan/oxidized pullulan composite film for postoperative wound sealing and localized cisplatin delivery in nasopharyngeal carcinoma. The amine groups in chitosan react with aldehyde groups in oxidized pullulan via Schiff base formation (C=N), generating a bioadhesive film. The film adheres to the nasopharyngeal surgical site, serving as a depot for sustained cisplatin release to inhibit tumor recurrence while simultaneously sealing the wound

As shown in Figure 3, the FTIR spectra of chitosan, oxidized pullulan, and the composite film were normalized to enable clearer comparison of key functional group peaks. The broad absorption band around 3400 cm^{-1}, attributed to O–H and N–H stretching, appeared in all three samples with slight intensity variation. Oxidized pullulan exhibited a prominent C=O peak near 1720 cm^{-1}, while chitosan showed a characteristic amide I band around 1650 cm^{-1}. Notably, the composite film displayed a distinct new peak centered at approximately 1630 cm^{-1}, which is not present in either raw material alone. This peak is assigned to the C=N imine bond formed via Schiff base reaction, indicating successful chemical crosslinking between the amine groups of chitosan and the aldehyde groups of oxidized pullulan. The normalized spectra clearly highlight this structural transformation, validating the formation of the designed bioadhesive network.

As shown in Figure 4, the lap-shear adhesion strengths of the three film types were quantitatively compared on wet sausage casing, simulating a mucosal surface. Chitosan and oxidized pullulan films exhibited moderate adhesion values of approximately 45 and 30 kPa, respectively. In contrast, the chitosan/oxidized pullulan composite film demonstrated a markedly higher adhesion strength of 55 kPa. The data are presented as mean ± standard deviation, with the composite group showing a statistically significant increase in bonding performance. The inset schematic illustrates the test configuration, where the film was sandwiched between two pieces of sausage casing and subjected to tensile loading. These results indicate that the Schiff base crosslinking structure formed between chitosan and oxidized pullulan substantially improves the cohesive and adhesive properties of the material under wet conditions.

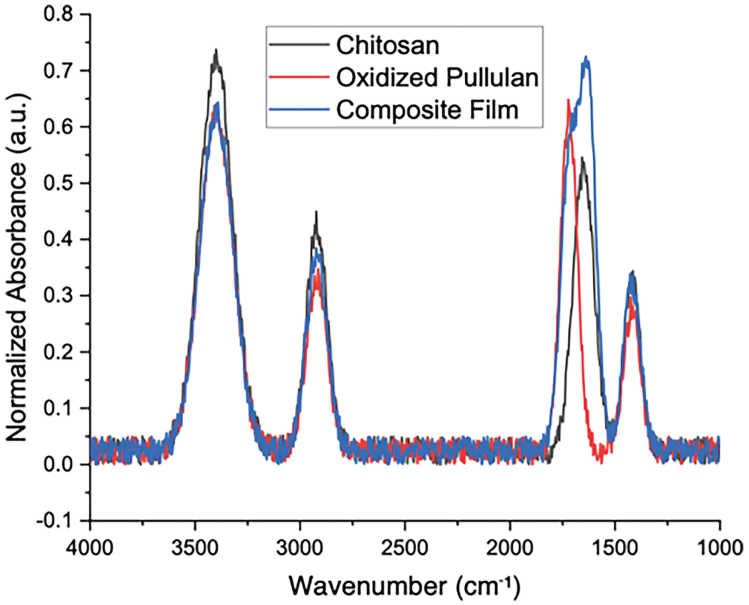

Figure 3. Normalized FTIR spectra of chitosan, oxidized pullulan, and the chitosan/oxidized pullulan composite film. Key absorption bands corresponding to O–H/N–H stretching (~3400 cm^{-1}), C–H stretching (~2920 cm^{-1}), C=O stretching (~1720 cm^{-1}), and C=N imine bond (~1630 cm^{-1}) are highlighted. Data were normalized to emphasize spectral differences between materials

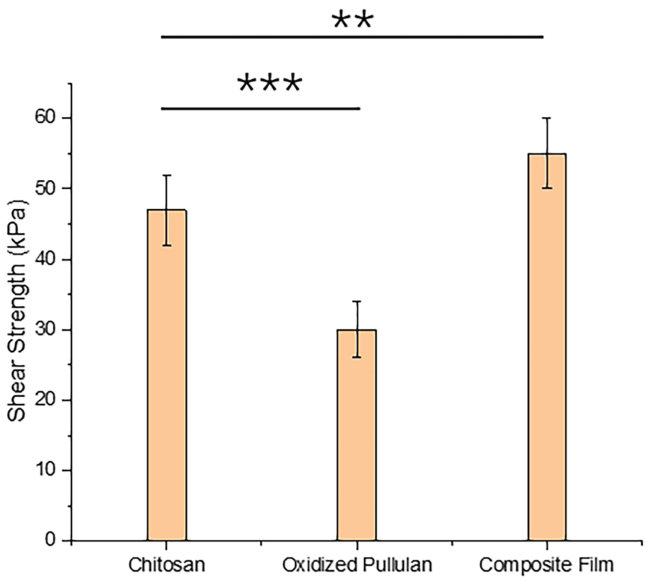

Figure 4. Lap-shear adhesion strength of chitosan, oxidized pullulan, and composite film measured on wet sausage casing substrate. The composite film exhibited significantly enhanced adhesion compared to the individual components. Inset: schematic of the lap-shear test configuration. $p < 0.01$ (**), and $p < 0.001$ (***)

As shown in Figure 1, ICP-MS analysis revealed a time-dependent cumulative release of cisplatin from the composite film. The release rate increased from 8.1% at 1 h to approximately 63.2% at 24 h, and reached 84.3% at 72 h. The release profile exhibited a biphasic pattern, with an initial burst phase

followed by a more gradual sustained release. Error bars represent standard deviations from triplicate measurements and indicate good reproducibility across all time points. As shown in Figure 5, treatment with free cisplatin and the cisplatin-loaded composite film extract significantly reduced the viability of CNE-2 cells compared to the control. The free cisplatin group resulted in approximately 42% cell viability, while the composite film loaded with cisplatin showed even stronger inhibitory effect, reducing viability to around 28%. In contrast, the drug-free composite film had minimal cytotoxicity, maintaining viability above 85%, comparable to the untreated control group. These results demonstrate that the film matrix itself is biocompatible, while the incorporation of cisplatin retains its cytotoxic activity against cancer cells. The lower viability observed with the cisplatin-loaded film suggests sustained and possibly enhanced local delivery compared to free drug exposure.

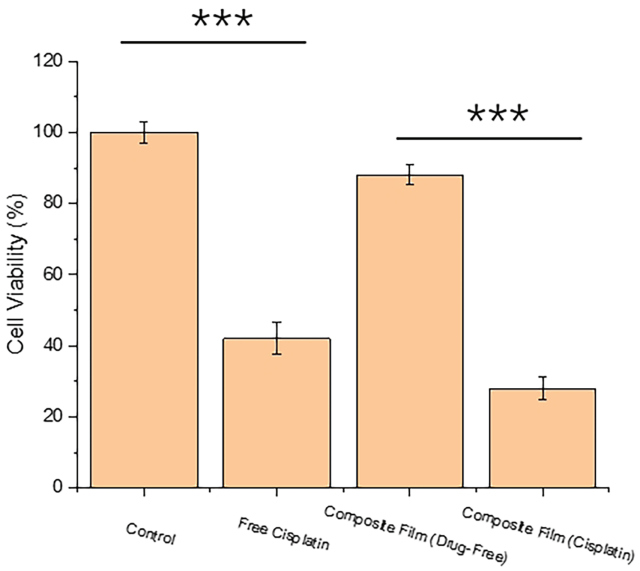

Figure 5. Cell viability of nasopharyngeal carcinoma cells (CNE-2) after treatment with free cisplatin, drug-free composite film extract, and cisplatin-loaded composite film extract for 48 h. Data are expressed as mean ± standard deviation (n = 3). $p < 0.001$ (***)

As shown in Figure 6, the real-time cell migration profiles revealed significant differences among treatment groups. The control group displayed a slow and steady increase in cell index over 48 h. Oxidized pullulan extract modestly enhanced migration compared to control, while chitosan extract showed a greater effect. Notably, the composite film extract led to a pronounced increase in cell index, with the steepest slope and highest final value, indicating the strongest promotion of cell migration. These results suggest that the combined material synergistically enhances epithelial cell motility, likely due to its favorable biochemical composition and microenvironmental support. The RTCA curves provide dynamic and quantitative evidence for the migration-promoting effect of the composite system.

4. Discussion

As shown in Figure 2, the chitosan/oxidized pullulan film system integrates molecular-level crosslinking and functional therapeutic delivery into a single platform for postoperative management of nasopharyngeal carcinoma. The Schiff base formation between chitosan and oxidized pullulan enhances the film's adhesiveness, especially under moist conditions typical of nasopharyngeal tissue, which is critical for stable fixation on surgical wounds. This adhesive property, combined with the biocompatibility of natural polysaccharides, enables the film to serve as an effective wound dressing [13]. Furthermore, the figure provides sustained release over 48 h *in vitro*, which may support

localized drug exposure. Further studies are needed to evaluate long-term release kinetics and systemic distribution [14]. Overall, the schematic in Figure 2 highlights the multifunctionality of the designed film and justifies its use as a dual-action material combining wound protection with sustained anti-cancer therapy [15].

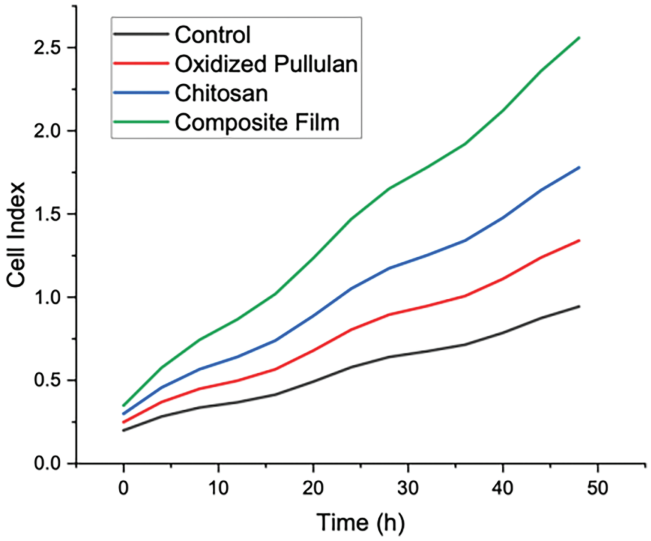

Figure 6. Real-time cell migration curves of nasopharyngeal epithelial cells (NP69) over 48 h in the presence of different material extracts, measured by impedance-based RTCA assay. The composite film group showed the highest cell index, indicating enhanced migratory activity

As shown in Figure 3, FTIR analysis confirms the formation of a Schiff base linkage in the composite film through the emergence of a characteristic C=N stretching band at ~1630 cm^{-1}. This spectral change is not evident in the individual chitosan or oxidized pullulan spectra, supporting the hypothesis that crosslinking occurs specifically during film formation [16]. Normalization of the FTIR data was applied to better distinguish overlapping peaks and emphasize critical differences in chemical structure. The reduction in C=O peak intensity in the composite compared to oxidized pullulan further suggests aldehyde consumption during the reaction. These findings provide direct molecular evidence for the covalent interaction between the two polysaccharides and validate the structural basis of the composite's adhesive properties [17,18].

As shown in Figure 4, the enhanced lap-shear adhesion of the composite film can be attributed to the synergistic effect of covalent crosslinking and interfacial compatibility. While chitosan provides intrinsic film-forming and bioadhesive properties, its interaction with oxidized pullulan through Schiff base chemistry generates a denser and more cohesive network. The wet adhesion test on sausage casing was used as a simplified model to mimic a moist biological interface under standardized conditions. While it provides initial insight into the material's adhesive potential in wet environments, we acknowledge that it does not replicate the structural or biochemical complexity of nasal or pharyngeal mucosa. Therefore, further validation using animal mucosal tissue or biomimetic substrates is necessary to assess clinical relevance more accurately. The composite film's superior adhesion performance suggests that the imine bond formation not only enhances mechanical strength but also promotes better interfacial bonding with biological substrates. These findings support the potential of this material as a robust wound sealing platform for postoperative use in nasopharyngeal carcinoma [19,20].

The ICP-MS-based drug release profile shown in Figure 1 confirms that the composite film can provide prolonged cisplatin release over 72 h. Compared with preliminary UV–Vis data, the ICP-MS quantification offers improved accuracy and reliability, especially at lower concentrations. The observed

biphasic pattern likely results from rapid diffusion of surface-associated drug in the early phase and matrix-controlled release thereafter. This sustained release behavior is consistent with the formation of a hydrated, crosslinked polymer network via Schiff base chemistry, which limits drug mobility. The relatively small standard deviations further support the reproducibility and structural stability of the release system, validating its suitability for localized chemotherapeutic delivery [21].

As shown in Figure 5, the composite film exhibits dual functionality, with excellent biocompatibility and effective antitumor activity upon cisplatin loading [3]. The high cell viability in the drug-free film group confirms that the chitosan/oxidized pullulan matrix is non-toxic to nasopharyngeal carcinoma cells, making it suitable as a biomedical material [22]. The significant reduction in viability in the cisplatin-loaded film group indicates that the released drug retains its bioactivity and is efficiently delivered to cells. Notably, the lower viability observed in the composite film group compared to the free drug group suggests that sustained release may enhance drug accumulation or prolong cytotoxic exposure. These results support the potential of the film system for localized chemotherapeutic applications following surgical resection [23,24].

As shown in Figure 6, the composite film significantly enhanced the migration of nasopharyngeal epithelial cells in a time-dependent manner, outperforming both individual component extracts and the control. The cisplatin concentration in the extract solution used for cell assays was not directly quantified, which limits the comparability to the free cisplatin group treated at a fixed concentration. As a result, cytotoxicity data should be interpreted qualitatively rather than as a dose-controlled comparison. The impedance-based RTCA platform allowed real-time monitoring of migratory behavior without labeling, providing sensitive detection of subtle differences. The observed increase in cell index in the composite group suggests that the chitosan/oxidized pullulan matrix not only maintains biocompatibility but actively promotes cell movement. This may be attributed to the hydrated polymer network, Schiff base crosslinking, and moderate degradation byproducts that support cellular activity [25]. These findings suggest that the composite film extract may stimulate epithelial cell migration *in vitro*. However, whether this effect translates into a beneficial wound healing response requires further investigation. It remains necessary to evaluate the influence of degradation products on inflammatory signaling and long-term epithelial behavior in more comprehensive biological models [26].

5. Conclusion

In this study, a chitosan/oxidized pullulan composite film was developed through Schiff base crosslinking, and its potential for postoperative application in nasopharyngeal carcinoma was preliminarily evaluated. The film demonstrated satisfactory wet adhesion strength, sustained cisplatin release behavior, good cytocompatibility, and moderate inhibitory effects on nasopharyngeal carcinoma cells. In addition, extract-based assays indicated a potential for promoting epithelial cell migration *in vitro*. These findings suggest that the composite film shows potential as a dual-function material for localized drug delivery and wound sealing at the *in vitro* level. However, the current study does not include *in vivo* validation. Further work involving mucosal adhesion models, animal studies, and long-term biocompatibility assessments is needed before considering any clinical application. Future studies may also explore formulation optimization and integration with other therapeutic agents to broaden its applicability.

Acknowledgement: Not applicable.

Funding Statement: The study was supported by Ningbo Clinical Research Center for Otolaryngology Head and Neck Disease (2022L005), Ningbo Top Medical and Health Research Program (2023030514) and Zhejiang Provincial Medical and Health Science Research Foundation (2025KY221) with Bing Cao.

Author Contributions: All authors contributed to this present work: [Bing Cao] designed the study, [Shanshan Gu] acquired the data, [Yi Hu] interpreted the data. [Yuna Zhang] drafted the manuscript,

[Bing Cao] revised the manuscript. All authors reviewed the results and approved the final version of the manuscript.

Availability of Data and Materials: The datasets generated and/or analyzed during the current study are available from the corresponding author Bing Cao upon reasonable request.

Ethics Approval: Not applicable.

Conflicts of Interest: The authors declare no conflicts of interest to report regarding the present study.

References

1. The Medical Letter. Toripalimab (loqtorzi) for nasopharyngeal carcinoma. Med Lett Drugs Ther. 2024;66(1694):e16–7. doi:10.58347/tml.2024.1694e.
2. Araujo LFS, Ferreira CRDN, de Araújo GS, Araújo AJ, Marinho-Filho JDB, Lima ABN, et al. Effective dressing: development of N-carboxyethyl chitosan/oxidized locust bean gum scaffolds. ACS Omega. 2025;10(16):16717–30. doi:10.1021/acsomega.5c00521.
3. Zhang B, Mai H, Liang X, Liu Y, Huang W. Carboxymethyl chitosan/oxidized sodium alginate self-healing emulsion gels with enhanced physical stability. Food Hydrocoll. 2025;166:111336. doi:10.1016/j.foodhyd.2025.111336.
4. Hsieh HT, Zhang XY, Wang Y, Cheng XQ. Biomarkers for nasopharyngeal carcinoma. Clin Chim Acta. 2025;572:120257. doi:10.1016/j.cca.2025.120257.
5. Bayatfard P, Sari SY, Yazici G. Chemotherapy, radiation therapy, and nasopharyngeal carcinoma. JAMA Oncol. 2024;10(9):1292. doi:10.1001/jamaoncol.2024.2519.
6. Bikiaris RE, Tsamesidis I, Kontonasaki E, Baciu D, Steriotis T, Charalambopoulou G, et al. Chitosan/oxidized-dextran dressings containing mesoporous bioglass nanoparticles for hemostatic applications. J Mater Sci. 2024;59(37):17593–608. doi:10.1007/s10853-024-10241-2.
7. Hidaka M, Sakai S. Photo- and schiff base-crosslinkable chitosan/oxidized glucomannan composite hydrogel for 3D bioprinting. Polysaccharides. 2025;6(1):19. doi:10.3390/polysaccharides6010019.
8. Cheng F, He J, Yan T, Liu C, Wei X, Li J, et al. Antibacterial and hemostatic composite gauze of N, O-carboxymethyl chitosan/oxidized regenerated cellulose. RSC Adv. 2016;6(97):94429–36. doi:10.1039/c6ra15983d.
9. Chetouani A, Elkolli M, Bounekhel M, Benachour D. Chitosan/oxidized pectin/PVA blend film: mechanical and biological properties. Polym Bull. 2017;74(10):4297–310. doi:10.1007/s00289-017-1953-y.
10. Dragan ES, Ghiorghita CA, Dinu MV, Duceac IA, Coseri S. Fabrication of self-antibacterial chitosan/oxidized starch polyelectrolyte complex sponges for controlled delivery of curcumin. Food Hydrocoll. 2023;135:108147. doi:10.1016/j.foodhyd.2022.108147.
11. Du X, Liu Y, Wang X, Yan H, Wang L, Qu L, et al. Injectable hydrogel composed of hydrophobically modified chitosan/oxidized-dextran for wound healing. Mater Sci Eng C Mater Biol Appl. 2019;104:109930. doi:10.1016/j.msec.2019.109930.
12. Guzel C, Munevveroglu S, Erten FD. Nasopharyngeal carcinoma masquerading as temporomandibular disorder. J Craniofacial Surg. 2024;35(8):e778–80. doi:10.1097/scs.0000000000010613.
13. Zhang L, Shen B, Zheng C, Huang Y, Liang Y, Fei P, et al. Chitosan/oxidized sodium alginate/Ca^{2+} hydrogels: synthesis, characterization and adsorption properties. Food Hydrocoll. 2024;156:110368. doi:10.1016/j.foodhyd.2024.110368.
14. Karati D, Kumar D. Molecular insight into the apoptotic mechanism of cancer cells: an explicative review. Curr Mol Pharmacol. 2024;17:e18761429273223. doi:10.2174/0118761429273223231124072223.

15. Jiang A, Ding H, Fu Y. Wogonin inhibits nasopharyngeal carcinoma cells. Curr Top Nutraceutical Res. 2024;22(1):64–73. doi:10.37290/ctnr2641-452x.22:.
16. Ko ES, Kim C, Choi Y, Lee KY. 3D printing of self-healing ferrogel prepared from glycol chitosan, oxidized hyaluronate, and iron oxide nanoparticles. Carbohydr Polym. 2020;245:116496. doi:10.1016/j.carbpol.2020.116496.
17. Li X, Kong X, Zhang Z, Nan K, Li L, Wang X, et al. Cytotoxicity and biocompatibility evaluation of N,O-carboxymethyl chitosan/oxidized alginate hydrogel for drug delivery application. Int J Biol Macromol. 2012;50(5):1299–305. doi:10.1016/j.ijbiomac.2012.03.008.
18. Lim DV, Woo WH, Lim JX, Loh XY, Soh HT, Lim SYA, et al. Targeting mutant-p53 for cancer treatment: are we there yet? Curr Mol Pharmacol. 2023;17:e140923221042. doi:10.2174/1874467217666230914090621.
19. Lin P, Liu L, He G, Zhang T, Yang M, Cai J, et al. Preparation and properties of carboxymethyl chitosan/oxidized hydroxyethyl cellulose hydrogel. Int J Biol Macromol. 2020;162:1692–8. doi:10.1016/j.ijbiomac.2020.07.282.
20. Liu YP, Feng ZK, Huang HQ, Wu WB, You R, Chen MY. Nasopharyngeal endoscopic submucosal dissection (NESD) for stage I nasopharyngeal carcinoma. Laryngoscope. 2025;135(7):2261–6. doi:10.1002/lary.32066.
21. Long LY, Hu C, Liu W, Wu C, Lu L, Yang L, et al. Microfibrillated cellulose-enhanced carboxymethyl chitosan/oxidized starch sponge for chronic diabetic wound repair. Mater Sci Eng C Mater Biol Appl. 2022;135:112669. doi:10.1016/j.msec.2022.112669.
22. Yuan Y, Ye F, Wu JH, Fu XY, Huang ZX, Zhang T. Early screening of nasopharyngeal carcinoma. Head Neck. 2023;45(10):2700–9. doi:10.1002/hed.27466.
23. Shen Y, Wang Z, Wang Y, Meng Z, Zhao Z. A self-healing carboxymethyl chitosan/oxidized carboxymethyl cellulose hydrogel with fluorescent bioprobes for glucose detection. Carbohydr Polym. 2021;274:118642. doi:10.1016/j.carbpol.2021.118642.
24. Nassif SJ, Michel EG, Scott AR, Tracy L, Tracy JC. Acquired nasopharyngeal stenosis after radiation treatment for nasopharyngeal carcinoma. Am J Otolaryngol. 2023;44(3):103819. doi:10.1016/j.amjoto.2023.103819.
25. Wu L, Li L, Pan L, Wang H, Bin Y. MWCNTs reinforced conductive, self-healing polyvinyl alcohol/carboxymethyl chitosan/oxidized sodium alginate hydrogel as the strain sensor. J Appl Polym Sci. 2021;138(6):49800. doi:10.1002/app.49800.
26. Wang Z, Zhao Y, Zhang L. Emerging trends and hot topics in the application of multi-omics in drug discovery: a bibliometric and visualized study. Curr Pharm Anal. 2024;21(1):20–32. doi:10.1016/j.cpan.2024.12.001.

Received: 28 August 2025; Accepted: 13 November 2025